A COMPARATIVE EVALUATION OF THE COASTAL INTERNAL BOUNDARY-LAYER HEIGHT EQUATIONS

M. STUNDER and S. SETHURAMAN

Department of Marine, Earth and Atmospheric Sciences, North Carolina State University, Raleigh, NC 27695, U.S.A.

(Received in final form 21 September, 1984)

Abstract. A parabolic shaped Thermal Internal Boundary Layer (TIBL) develops at the coast because of the temperature discontinuity between land and water. The TIBL is shown to play a significant role in determining where a coastal elevated plume fumigates to the ground. Six TIBL models available in the literature were identified and statistically compared. Two data bases obtained from the TIBL experiments, one at eastern Long Island, the other at the Kashimaura area of Japan, were used for statistical comparisons. Statistical methods of t, F and R were used to determine bias, scatter and correlation. The data were also classified according to wind speed (low and high) and stability (unstable, neutral, isothermal and stable onshore flow) to determine whether some models worked better under certain conditions. These limited data indicated that a formulation which included heat flux and wind speed together with overwater lapse rate, all raised to the half power, performed the best. Classifications according to wind speed and thermal stability also showed that the heat flux type of equation worked reasonably well.

1. Introduction

The growth of industrial and commercial operations near shorelines has created a need over the past several years for dispersion models that can handle the unique meteorological conditions present in the coastal environment. Expansion of oil handling and drilling facilities, mineral and chemical processing plants, fossil fuel plants and increased concern over nuclear power plants have created a need, from both regulatory and emergency response planning viewpoints, for continued refinements of existing models and the development of new models.

A reasonably thorough treatment of the atmospheric processes present in a coastal area can be included in a numerical model but such models are rarely used for operational purposes due to their complexities. There are several statistical models (Lyons and Cole, 1973; Schuh, 1975; Van Dop *et al.*, 1979; Misra, 1980) which compute ground-level concentrations based on the assumptions of Gaussian distribution or mixed-layer hypothesis. An important component of all these coastal fumigation models is the Thermal Internal Boundary Layer (commonly called TIBL) that usually originates at the land-water interface and thickens downwind. Interaction between the TIBL and the plume from an elevated source at the coastline influences the distribution of ground-level concentration downwind and the location of its maximum value.

2. TIBL Dynamics

Internal boundary layers (IBLs) develop near a coastline due to differences in the physical properties of land and water. A mechanically-forced IBL develops from the

Boundary-Layer Meteorology **32** (1985) 177–204. 0006–8314/85.15.

change in shear stress because of the roughness discontinuity present at the shoreline. The thickness of this roughness IBL has been shown to grow at a rate of about 1:10 with respect to downwind distance (Elliot, 1958). The roughness IBL is generally dominated, however, by thermal effects of the surface discontinuity (Raynor *et al.*, 1979). Other definitions of coastal IBLs pertain to discontinuities in specific humidity and momentum (Gamo *et al.*, 1982).

A free convective IBL forms due to the differences in temperature between land and water (hence the name 'Thermal' Internal Boundary Layer). The formation of the TIBL based on flow adjustment theory has been given by various authors (Kerman *et al.*, 1982; Lyons, 1975). An airmass advected over a cool lake or ocean surface is not destabilized by convective elements as would an overland airmass. Instead, the marine air mass cools from below via conduction from the water's surface and thus becomes stable. As the stable marine air mass crosses the shoreline (i.e., onshore flow), it must adjust, first in the lowest levels, then in the higher levels, to the resulting discontinuity in temperature. This adjustment is accomplished by the generation of turbulence which acts as a transport mechanism for surface heat from the land surface. The TIBL interface generally slopes upward from the coastline until at some point downwind (X) it assumes an 'equilibrium height' which is the height of the inland mixed layer. The adjustment of the once stable onshore flow is complete at this equilibrium height.

The TIBL can be classified by stability into two broad categories, for descriptive purposes, as shown in Figure 1a. Category I TIBLs are characterized by overwater stable lapse rates. In this case the TIBL growth begins at the shoreline ($X = 0$) and continues until an equilibrium point is reached downwind. Category II TIBLs are characterized by overwater stabilities that are near-neutral. In this case the TIBL does not begin at the coastline but instead grows out of the marine neutral layer with some initial height h_0 as shown in Figure 1b.

Several definitions of the height of the TIBL interface are given in the literature. Venkatram (1977) defines the TIBL interface as being the point where a temperature profile jump occurs (i.e., a change in stability from neutral to stable). Anthes (1978) in his numerical sea breeze model follows Venkatram's general TIBL interface definition and defines the TIBL height (h) as being the first level greater than 180 m above the ground at which the potential temperature gradient exceeds 1 °C km^{-1}.

Lyons (1975) defined the TIBL height as being the average maximum height to which turbulent penetrative convective elements are reaching at a given place and time. Lyons (1975) presented turbulence data to illustrate the sharp change of turbulence across the TIBL interface. An analysis of the variation of σ_w with height for several coastal cases (SethuRaman *et al.*, 1982) shows turbulence variations of a factor of 5 across the TIBL interface. Other investigators (Raynor *et al.*, 1979; Gamo *et al.*, 1983) have also found sharp turbulence changes across the TIBL interface.

Gamo *et al.* (1982) have investigated the variation in h based on the two definitions and have concluded that the interface defined by turbulence is 1.4 times higher than the interface defined by temperature. A similar result was obtained by Raynor *et al.* (1979). In this paper we adopt the more common turbulence definition of TIBL height.

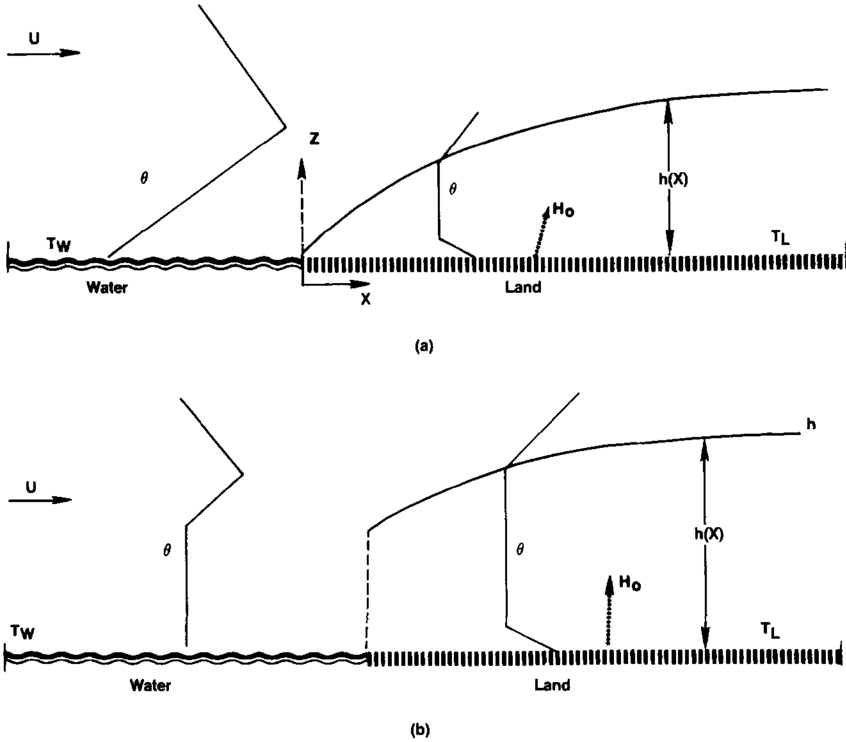

Fig. 1(a). Typical TIBL structure with stable onshore flow. (b). Typical TIBL structure with neutral onshore flow.

It is important to note that the TIBL can develop in either sea breeze or gradient flow regimes. TIBLs can also begin a few kilometers offshore in response to warm water pockets creating the necessary atmospheric thermal discontinuity. Finally, TIBLs can form in an offshore breeze if there is a sufficient land-water temperature contrast.

The structure of the TIBL in terms of its height and vertical variation of wind and temperature within it will be governed by the mesoscale phenomena both upwind and downwind of the coast.

3. Review of the TIBL Height Prediction Equations

A review of the literature indicates several approaches in determining the TIBL height. A historical flow chart of TIBL equation development is presented in Figure 2. Early efforts in specifying the TIBL height are given by Van der Hoven (1967) based on work done by Prophet (1961). The general equation is:

$$h = 8.8\left(\frac{X}{U\Delta\theta}\right)^{1/2} \qquad (1)$$

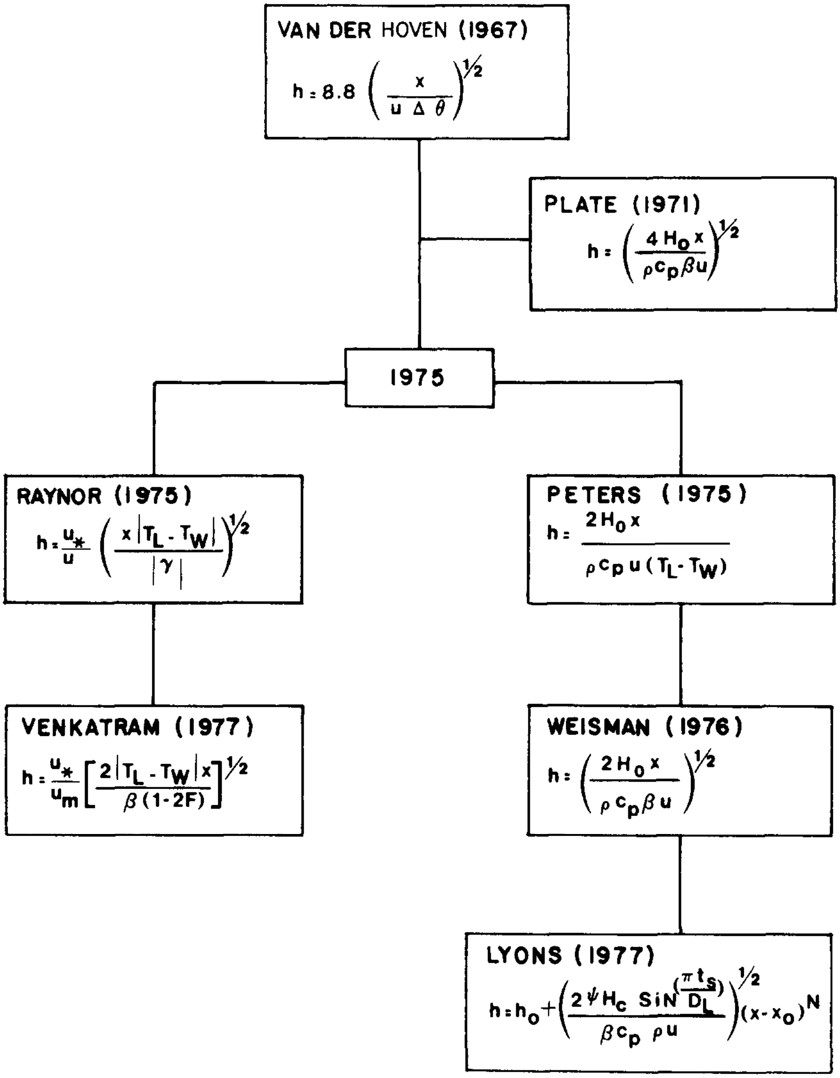

Fig. 2. Historical flow chart showing TIBL equation development.

where

h = TIBL height (m).

X = Distance downwind from the land-water interface (m).

U = Mean wind speed in TIBL (m s^{-1}).

$\Delta\theta$ = Temperature difference between the top and bottom of the overwater surface-based inversion (deg C).

The relationship was empirically derived to fit observational data and is not dimensionally homogeneous. The importance of the upwind stability generally characterized by the $\Delta\theta$ term and the parabolic dependence on downwind distance were first recognized in this formulation.

The first of two recent approaches involves the work of Raynor *et al.* (1975) and Venkatram (1977). Raynor *et al.* (1975) derived an equation of the following form based on physical and dimensional considerations:

$$h = \frac{u_*}{U}\left\{\frac{X|T_L - T_W|}{|\gamma|}\right\}^{1/2} \tag{2}$$

where

u_* = Downwind surface frictional velocity.
T_L = Downwind surface temperature (land).
T_W = Upwind surface temperature (water).
γ = Absolute lapse rate upwind.
U = Mean wind speed at a height of 10 m downwind.

The equation is dimensionally homogeneous and incorporates the use of land-water temperature difference. The vertical structure of TIBL turbulence (and therefore the TIBL height) has been shown to depend significantly on the land-water temperature differential (SethuRaman *et al.*, 1982). A drag coefficient parameterization, u_*/U, was incorporated into Equation (2) to account for the change in surface roughness.

Equation (2) does not directly take into account the surface heat flux over land which is important in the convective growth of the TIBL. Another problem is singularity as $\gamma \to 0$ in the near-isothermal overwater condition.

The TIBL has been treated analytically as a horizontally inhomogeneous mixed layer in a steady state condition by several authors (Venkatram, 1977; Gamo *et al.*, 1983). By considering the TIBL as being two-dimensional, the mixed-layer energy equation can be written following Venkatram's (1977) notation as:

$$hU_m \frac{\partial\theta_m}{\partial X} = (\overline{w'\theta'})_0 - (\overline{w'\theta'})_i \tag{3}$$

where

U_m = Mixed-layer mean wind.
θ_m = Mixed-layer mean potential temperature.
$(\overline{w'\theta'})_{0,i}$ = Heat flux at the surface and at the TIBL height h, respectively.

A simplified entrainment hypothesis yields:

$$\Delta\theta = F\gamma h \tag{4}$$

where F is an entrainment fraction and $\Delta\theta$ is the temperature jump across the TIBL. The ratio of $-(\overline{w'\theta'})_i$ to $(\overline{w'\theta'})_0$ has been shown to equal a constant C (Betts, 1973) where C is also equal to $F/(1 - 2F)$.

From Figure 1a an expression for h can be graphically determined so that:

$$h = \theta_m - \theta_w + \Delta\theta = \gamma h. \tag{5}$$

Using Equation (4) in (5),

$$h = \frac{\theta_m - \theta_w}{\gamma(1 - F)}. \tag{6}$$

Following Venkatram (1977) and using parameterizations for the surface heat flux and substituting (4) and (6) into (3), we obtain:

$$h = \frac{u_*}{u_m}\left[\frac{2\,|T_L - T_W|X}{\beta(1 - 2F)}\right]^{1/2} \tag{7}$$

where β is the potential temperature gradient over water.

Equation (7) assumes that the TIBL is dominated by buoyancy. In addition, equation (7) assumes that the layer is well-mixed and therefore produces uniform vertical potential temperature profiles and velocity gradients. The well-mixed assumption may not hold under all conditions as shown by SethuRaman (1982). For strongly stable upwind conditions with a surface-based inversion, a low-level super-geostrophic jet is usually found over the ocean. This layer is not completely mixed over land within the TIBL downwind. Super-geostrophic wind velocities are observed over land in the coastal region in spite of convective conditions. Equation (2) derived from dimensional and physical considerations and Equation (3) derived analytically are essentially similar except for the entrainment variable F (~ 0.2) which increases the estimates of h by a factor of about two.

Peters (1975) developed a scheme of determining TIBL height with the assumption that the upward turbulent transport of energy in the boundary layer causes a temperature gradient which corresponds to a constant near-ground vertical heat flux. The average overland TIBL temperature may be written as:

$$T_A = \tfrac{1}{2}(T_W + ah + T_L) \tag{8}$$

where

T_A = Average temperature of the TIBL layer.

a = constant.

Peters (1975) defines $T_W + ah$ as being representative of the temperature profile over both land and water. Equation (8) therefore relates the TIBL layer temperature obtained over a given width of land bounded by height h to the heating of the air passing over that width of land. An energy balance performed on the area under h yields the following:

$$H_0 X = \rho c_p U\,[\tfrac{1}{2}(T_W + ah + T_L) - \tfrac{1}{2}(T_W + T_W + ah)]h \tag{9}$$

where

H_0 = surface heat flux over land;

c_p = specific heat at constant pressure (0.24 cal g^{-1} k^{-1}); and

ρ = density of air (1.2×10^3 gm^{-3}).

The first term on the right side of Equation 9 is the average overland TIBL temperature as given in Equation 8 and the second term is the average overwater temperature over a height equal to h.

Solving for h, Peters (1975) obtained

$$h = \frac{2H_0X}{\rho c_p U(T_L - T_W)}. \tag{10}$$

The linear nature of Equation (10) implies that Peters' (1975) scheme should predict a fast growing TIBL. In addition, this model can not be used for large downwind distances where the nearshore initial stable stratification has dissipated.

Plate (1971) using earlier work by Ball (1960) derived an equation for the height of the free convective boundary layer capped by a stable layer. He assumed that the heat flux at the top of the TIBL is equal to the surface heat flux so that:

$$(\overline{w'\theta'})_h = (\overline{w'\theta'})_0 \tag{11}$$

where subscripts h and 0 refer to the top of the TIBL and the surface respectively.

If we also assume a constant surface heat flux and sharp temperature discontinuity at the TIBL interface then using the geometry of assumed thermal structure (see Plate, 1971), total heat input can be written as:

$$h\frac{\mathrm{d}T}{\mathrm{d}t} + (T_L + \beta h - T)\frac{\mathrm{d}h}{\mathrm{d}t} = \frac{2H_0}{\rho c_p} \tag{12}$$

where T = temperature at some height.

Assuming that the temperature change and TIBL thickness are proportional,

$$\alpha\frac{\mathrm{d}h}{\mathrm{d}t} = \frac{\mathrm{d}T}{\mathrm{d}t} \tag{13}$$

and

$$\alpha h = T - T_L \tag{14}$$

where α is an arbitrary constant. By combining Equations (12), (13), and (14) and solving algebraically for h, Plate (1971) obtained the following:

$$\beta h^2 = \frac{2H_0 t}{\rho c_p} \tag{15}$$

which yields,

$$h = \left(\frac{4H_0X}{\rho c_p \beta U}\right)^{1/2}. \tag{16}$$

Weisman (1976) suggested using an equation similar to (16) as a parabolic extension to Peters' (1975) Equation (10). It is not clear how this equation was derived. The Weisman equation is:

$$h = \left(\frac{2H_0X}{\rho c_p \beta U}\right)^{1/2} \tag{17}$$

Alternatively, Gamo *et al.* (1983) have derived (17) from a mixed-layer theory. Gamo *et al.* (1983) assumed that the TIBL is heated uniformly and that the heat flux decreased linearly with height such that:

$$U\frac{\partial\theta(x)}{\partial x} = \frac{-1}{\rho c_p}\frac{\partial H(x,z)}{\partial z}. \tag{18}$$

Ignoring the temporal variation of θ and horizontal variation of heat flux, Gamo *et al.* (1983) integrated Equation (18) with the boundary conditions $H = H_0$ at $z = 0$ and $H = 0$ at $z = h$ and obtained Equation (17).

There are two practical problems in using (17). The determination of H_0 is difficult in most meteorological applications. Secondly, the signularity question arises as $\beta \rightarrow 0$ in the near-neutral case. In addition, for operational use, Weisman (1976) selected 100 cal/m^2 to fit the measured TIBL data to the predictive equation, yet it is commonly known that H_0 varies with time of day, latitude and cloud cover.

Lyons *et al.* (1983) have modified Equation (17) to account for the time dependence of H_0 by introducing various parameters such as a solar insolation factor and elapsed time since sunrise. The use of this heat flux parameterization closely follows the heat flux scheme used in a numerical sea breeze model by Anthes (1978).

The modified Weisman formulation (Equation (17)) given by Lyons *et al.* (1983) is:

$$h = h_0 + \left\{\frac{2\psi H_c \sin\left(\frac{\pi t_s}{D_L}\right)}{\beta c_p \rho U}\right\}^{1/2} (X - x_0)^N \tag{19}$$

where

ψ = solar insolation factor which was chosen arbitrarily as 0.1, 0.3, 0.6, and 1.0 for negligible, low, moderate and strong insolation, respectively,

H_c = 20% of the solar constant,

t_s = time since sunrise,

D_L = length of day,

N = a variable exponent,

h_0 = initial depth of TIBL – allows for TIBL growing out of neutral or unstable offshore layers,

x_0 = correction distance factor that accounts for changes in TIBL shape.

Once again Equation (19) has a singularity problem with $\beta \rightarrow 0$.

Additional problems result from questions in determining ψ, x_0, and N. Lyons *et al.* (1983), for example, determined N to be 0.61 based on the average of the 'best fit' N for four TIBL cases with x_0 = 2 km. This value may be highly site-dependent. It appears from different analytical and dimensional approaches (Plate, 1971; Venkatram, 1977; Raynor *et al.*, 1979) that N is equal to 0.5.

Finally, it is important to note that some coastal dispersion modelers (Van Dop *et al.*, 1979; Misra, 1980) prefer to simplify the TIBL equations such that:

$$h = AX^{1/2} \tag{20}$$

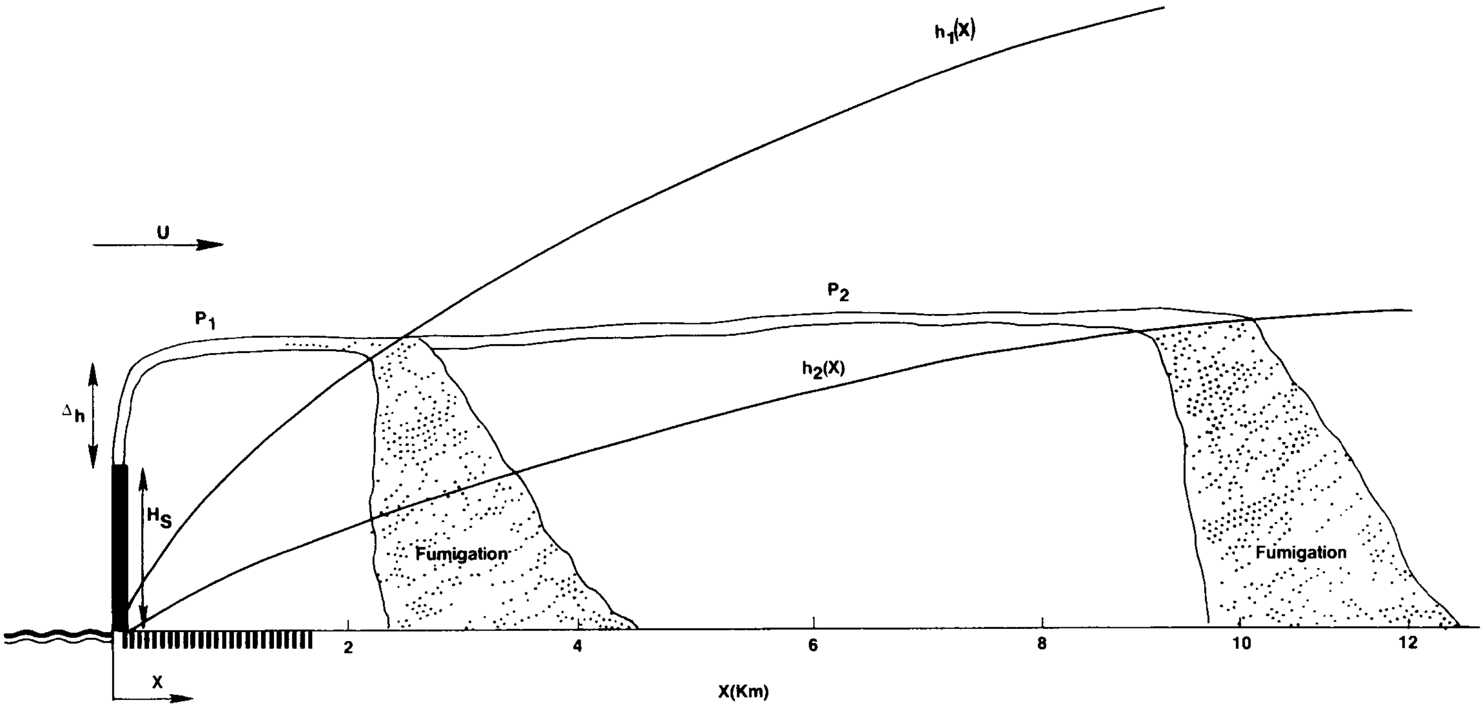

Fig. 3. The effects of TIBL variation on plume fumigation. P1 and P2 represent plume segments. $h_1(X)$ and $h_2(X)$ represent two different TIBL heights. H_s is the stack height, Δh is the plume rise, U is the wind speed (onshore) and X is the downwind distance from the shoreline.

where A = a factor containing different physical parameters necessary for TIBL determination. In the case of Equation (17) for example: $A = (2H_0/\rho c_p \beta U)^{1/2}$. Values of A were estimated by these investigators from actual measurements of the height of the TIBL at a given location. The importance of the variation of the TIBL upon coastal dispersion is discussed in the next section.

4. The Impact of TIBL Variation on Coastal Dispersion

Two important physical processes concerning dispersion in coastal regions are fumigation and trapping. Plumes emitted into the stable marine air at the shoreline ($X = 0$) normally move inland with onshore flow and at some point intersect the deepening TIBL. Intense downward mixing at the point of TIBL impaction can cause high ground-level concentration. Plumes have been observed to travel 20 to 30 km downwind before fumigating (Portelli, 1982).

Trapping conditions occur when stacks are located within the TIBL at some inland distance such that plumes are emitted into the convectively mixed TIBL and are effectively capped by the TIBL interface. If a plume is buoyant enough and a stack is located close to the TIBL interface, the plume may actually penetrate into the stable marine air and then fumigate back into the TIBL at a point of intersection farther downwind. The importance of TIBL variation on the fumigation case is illustrated with a practical example in Figure 3. Various parameters used in the figure are:

H_s = 160 m (stack height);
Δh = 90 m (plume rise);
U = 5 m sec^{-1};
$h_1(x) = 5.61\,(x)^{1/2}$ (maximum A factor used in Equation (20) – Misra and Onlock, 1982);
$h_2(x) = 2.71\,(x)^{1/2}$ (minimum A factor used in Equation (20) – Misra and Onlock, 1982).

We have chosen the maximum and minimum observed values of A from a fumigation experiment at the Nanticoke Power Generating Station on the northern shore of Lake Erie. The stack height for our example was selected arbitrarily. The TIBLs $h_1(x)$ and $h_2(x)$ were calculated using Equation (20).

For the case of $h_1(x)$, the TIBL grows sharply from the coast, reaching a height of about 250 m just after 2 km downwind. Fumigation of plume P1 begins at this point. For simplicity, we assume that plume P1 is mixed instantaneously into the TIBL. The fumigation zone is about 2 km long.

For the $h_2(x)$ case, the TIBL is seen to grow less sharply than for the $h_1(x)$ case. The TIBL height at 2 km is about 120 m, which is considerably below the effective stack height of 250 m. In this case, plume P2 impacts the shallow TIBL around 9 km downwind. Fumigation of plume P2 begins at this point.

The difference between h_1 (2 km) and h_2 (2 km) is about 130 m. This simple example illustrates that even a relatively small difference in predicting TIBL height at a given downwind distance may cause serious problems in predicting the location of the ground-level fumigation location and hence the location of maximum ground-level concentration. Every coastal dispersion model must therefore have a reliable TIBL variation module in order to predict the ground-level concentrations accurately.

5. TIBL Data Bases and Study Methodology

5.1. TIBL DATA BASES

We have identified seven TIBL data bases and reports from the literature and other sources. They are listed in Table I.

The most complete data bases in terms of overland, overwater and aircraft measurements are the eastern Long Island, and Kashimaura studies. We used these two data bases to evaluate various TIBL formulations.

TABLE I

Data base	Source
Brookhaven (BNL)	Raynor *et al.* (1979) and unpublished data
Kashimaura (Japan)	Gamo (1981), Gamo *et al.* (1982)
Nanticoke (Canada)	Lui (1977), Portelli (1982), Kerman *et al.* (1982)
Wisconsin/Lake Michigan	Lyons (1977)
Avon Lake/East Lake, Cleveland	unpublished data
Maine	Fritts *et al.* (1980)
Tampa Bay	unpublished data

5.2. METHODOLOGY

5.2.1. *BNL Data Base*

The Atmospheric Sciences Division of the Brookhaven National Laboratory investigated development and characteristics of the TIBL over Long Island, New York during the mid and late 1970s as part of their coastal meteorology program. Terrain of the study area varies from sandy near the coast to shrub and tree-covered farther inland.

Measurements of turbulence and temperature were made from aircraft and tower-mounted instruments. These data were plotted as a vertical cross-section by combining various heights along the flight track. Observations of land and ocean surface temperatures were made with an infra-red sensor from the aircraft. Flight tracks across Long Island are shown in Figure 4. For this study we chose tracks 3 and 4 since they provided the greatest overland distance for TIBL growth and were not influenced by inland bodies of water. Wind profiles were determined from pilot balloon soundings.

Methods for determining various parameters used in the TIBL equations are given in Table II. Wind speeds observed near BNL were used for overland values. A complete description of the experimental equipment is given by Raynor *et al.* (1979).

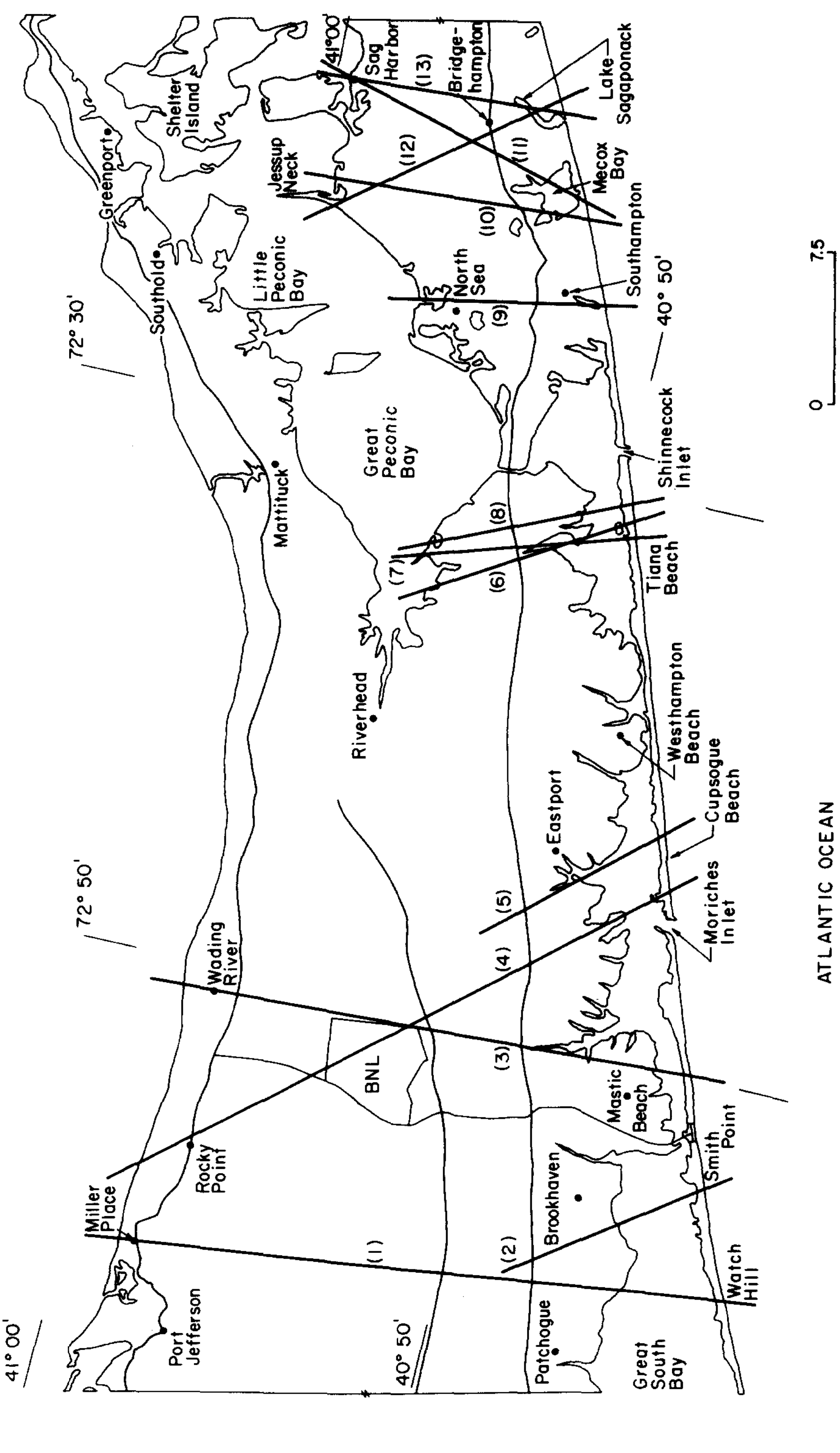

Fig. 4. Map of Long Island, New York showing principal flight tracks (numbered). Data from tracks (3) and (4) were examined in our study.

TABLE II

TIBL Parameters used for BNL Data Base

Parameter	Method
$U_{10,z}$	10 m winds from tower near BNL; U_z; wind profiles
$\Delta\theta$	Overwater temperature profiles (Balloon sounding, aircraft measurements overwater)
u_*	Assumed to be 0.5 m sec^{-1} (SethuRaman and Brinkman, 1983)
T_L	Infra-red sensor from aircraft
T_W	Infra-red sensor from aircraft
γ, β	Overwater temperature profiles
F	0.2 (Venkatram, 1977)
H_0	Surface similarity relationship $H_0 = \rho c_p u_* kz \frac{d\theta}{dz}$ where k is von Karman's constant (0.4) and z is the height over which temperature measurements were taken

5.2.2. *Kashimaura Data Base*

The Japanese National Research Institute for Pollution and Resources conducted a TIBL investigation in the Kashimaura–Kujukrihama region of Japan during the 1970's. We will refer to the study as Kashimaura for simplicity. The region is located 100 km east of Tokyo and is sandy with some shrubs and farmland. Figure 5 shows the triangular configuration of the coast. Occasionally, the Kashimaura sea breeze joined the Kujukurihama sea breeze. These cases were not considered in our analysis.

Aircraft measurements of turbulence and temperature were made from 50 m to 2000 m. Pilot balloon soundings were taken inland and at various points along the coast. Tower measurements of U and T were also made at several coastal and inland sites.

TABLE III

TIBL Parameters for Kashimaura Data Base

Parameters	Method
$U_{10,z}$	10 m winds from towers, U_z from pilot balloon wind profiles
$\Delta\theta$	Overwater aircraft traverses
u_*	$\sim \frac{\sigma_w}{1.3}$. σ_w values were obtained from overland aircraft flights at $z = 200$ m
T_L	IR sensors in overland aircraft
T_W	IR sensors in overwater aircraft
γ, β	Reconstruction of temperature profiles from overwater aircraft traverses
F	0.2 (Venkatram, 1977)
H_0	When H_0 was not given, the relationship $H_0 = 0.39S$, where S = solar insolation was used (Misra and Onlock, 1982)
ψ	Based on solar insolation data directly

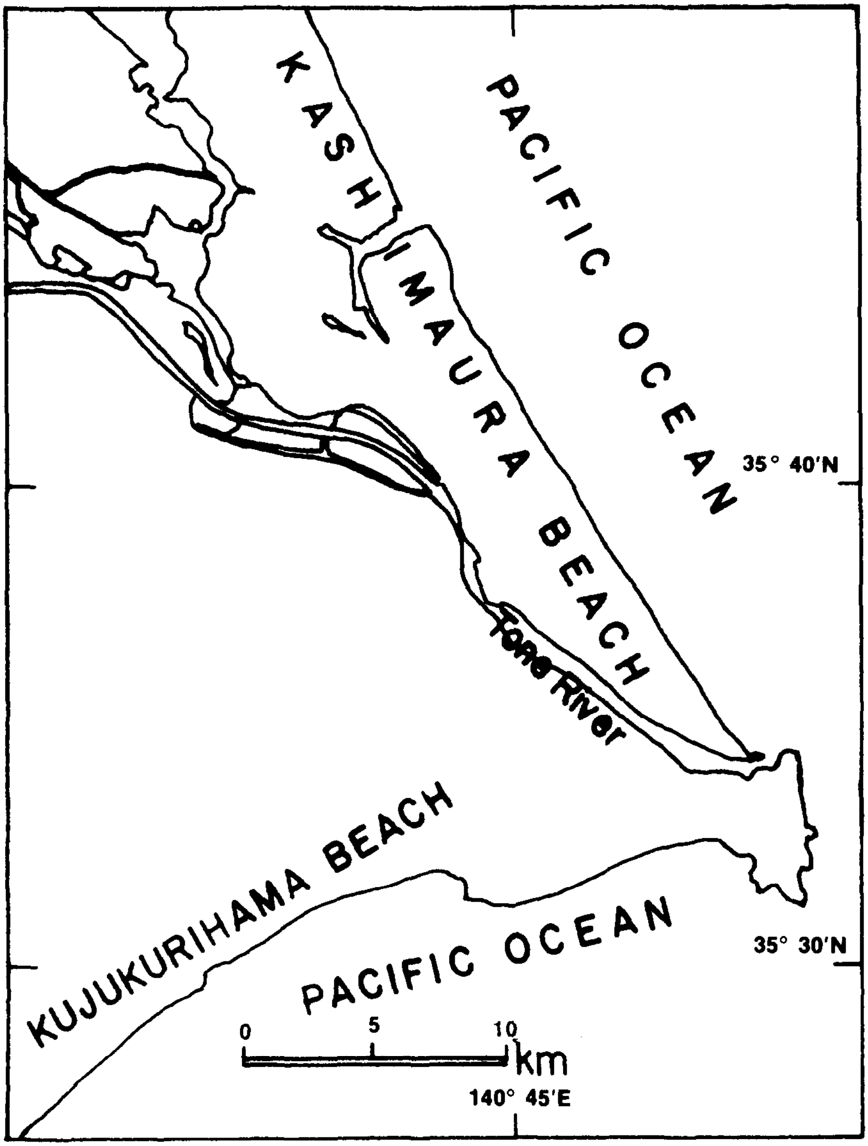

Fig. 5. Map of the Kashimaura–Kujukurihara coastal area of Japan. TIBL observations were taken on both the beaches.

Land and ocean surface temperatures (IR) were taken at 1 km intervals. Flight tracks were made across the entire region. Solar insolation data were available from the Choshi Observatory located at the apex of the triangle. Methods for determining the various TIBL parameters for this data base are listed in Table III. A complete description of the experimental methods is given by Gamo *et al.* (1982).

6. TIBL Equation Evaluation

We first present two typical cases (one with stable overwater conditions and one with unstable overwater conditions) to demonstrate some of the variations in the values obtained from TIBL prediction equations under different meteorological situations. The two data bases are then combined to describe the TIBL prediction equation variation in terms of an overall comparison. We conclude this section by categorizing the TIBL cases by stability and wind. Six TIBL formulas have been evaluated (Equations: (1), (2), (7), (10), (16), (17)).

Twenty-nine hours (cases) of TIBL measurements spanning 24 days were examined. The experiments were conducted during the period from March to November. Generally, each case contained between 4 and 12 TIBL measurements downwind. Observed TIBL heights were determined every 2 km downwind for the Kashimaura data base and every 1 km downwind for the BNL data base. The total number of observed TIBL heights for the 29 cases is 203.

6.1. Typical Cases of TIBL Variation

6.1.1. *Stable Conditions Upwind over Water*

The case presented here for evaluation is Brookhaven experiment #BL13 which was conducted on June 16, 1979 from 1330 to 1500 EST. A listing of the meteorological data pertaining to the experiment appears in Table IV. A surface-based inversion was present

TABLE IV

BNL #13 Meteorological Data

Parameter	Value
U	4.5 m s^{-1}
$\Delta\theta$	3.0 K
u_*	0.5 m s^{-1}
T_L	303 K
T_W	288.5 K
H_0	162 W m^{-2}
$\frac{dT}{dz}$	0.015 K m^{-1}
Wind direction	150°

over the water up to a level of 150 m. The water temperature was 14 K cooler than the land temperature. The presence of this strong temperature differential between the land and the water caused the TIBL to be shallow (less than 340 m high) since the warming of the marine air was gradual. TIBL observations continued out to 12 km downwind where an equilibrium height was approximately reached.

The predicted TIBL values for downwind distances up to 12 km are given in Figure 6. Figure 6 shows that for this case, Raynor's formulation (Equation (2)) predicts the TIBL

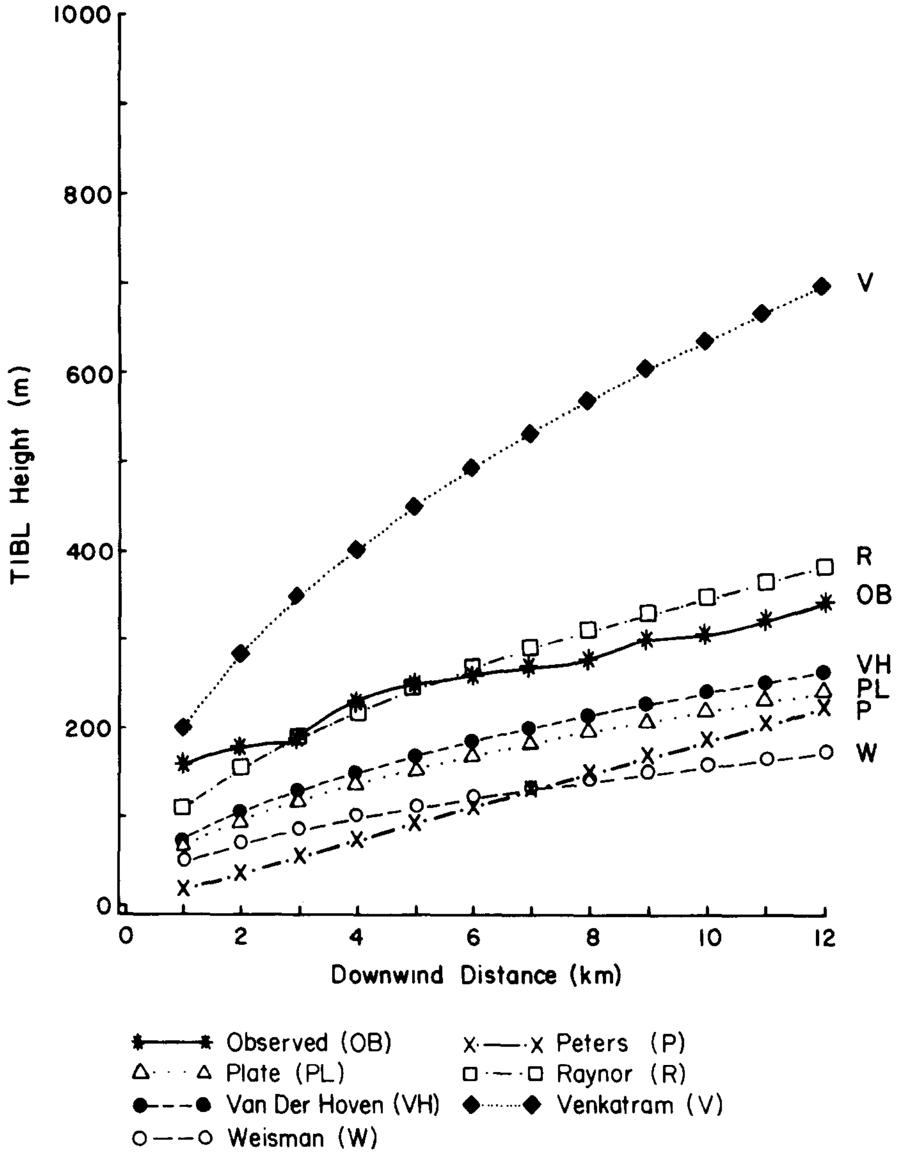

Fig. 6. Predicted and observed TIBL values for the onshore stable BNL BL# 13 case (June 13, 1978, 1530 EST)

height the best. Van der Hoven's equation (1) also predicts the TIBL height fairly well (within a factor of two) but tends to underpredict systematically. This may be because of the lack of TIBL forcing terms such as H_0, T_L, or T_W in his equation. Linear equation (10) of Peters (1975) underpredicts the TIBL height for all downwind distances. This could be attributed to the land-water temperature difference appearing in the denominator.

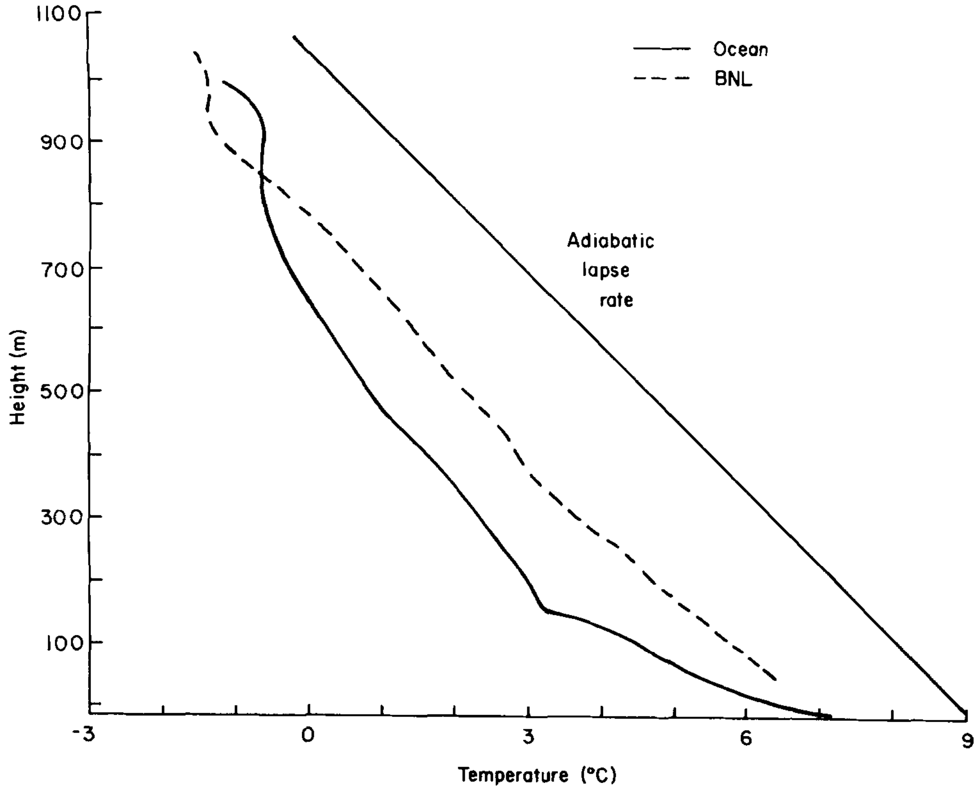

Fig. 7. Overland and overwater temperature profiles for the onshore neutral BNL BL # 6 case (March 18, 1975, 1200 EST)

Venkatram's formulation (Equation (7)) overpredicts the TIBL throughout. Much of this overprediction (as compared to the Raynor *et al.* (1975) formulation and observations) appears to have been created by the factor of 1.83 difference between the Venkatram term:

$$\left(\frac{2}{1 - 2F}\right)^{1/2} \tag{21}$$

where $F = 0.2$ (Venkatram, 1977) and the terms in the Raynor *et al.* formulation (Equation (2)). Weisman's equation underpredicts the TIBL height.

6.1.2. *Unstable Conditions Upwind over Water*

The case selected for unstable conditions was BNL # BL6 which occurred on March 18, 1975, 1130 to 1230 LT. A listing of the meteorological data pertaining to the experiment appears in Table V. The sounding shown in Figure 7 indicates that a shallow superadiabatic layer existed over the ocean near the surface capped by a stable layer. The TIBL equations were therefore modified by adding a constant h_0 to the original

TABLE V

BNL#6 Meterological Data

Parameter	Value
U	4.5 m s^{-1}
$\Delta\theta$	5.0 K
U_*	0.5 m s^{-1}
T_L	290.0 K
T_W	281.3 K
H_0	276. W m^{-2}
$\frac{dT}{dz}$	-0.0131 K m^{-1}
h_0	150 m: h_0 is the intial TIBL height due to unstable or near-neutral overwater conditions
Wind direction	150°

equation. For example, Equation (2) now becomes:

$$h = h_0 + \frac{u_*}{u}\left(\frac{X/T_L - T_W|}{|\gamma|}\right)^{1/2}. \tag{22}$$

We have to make this modification because the equations assume that offshore conditions are stable. The h_0 in this case was determined to be 150 m based on the overwater

TABLE VI

Comparison of h vs $h + h_0$

(km)	Observed TIBL (m)	TIBL	Van der Hoven	Raynor	Peters	Weisman	Venkatram	Plate
1	250	h	62	102	53	186	185	263
		$h + h_0$	212	252	203	336	335	413
2	450	h	88	146	105	263	262	372
		$h + h_0$	238	296	255	413	412	522
3	575	h	108	176	158	323	321	457
		$h + h_0$	258	326	308	473	471	607
4	600	h	124	204	211	373	371	527
		$h + h_0$	274	354	366	523	521	677
5	650	h	139	228	263	417	415	590
		$h + h_0$	289	378	413	567	565	740
6	700	h	152	250	316	456	454	645
		$h + h_0$	302	400	466	606	604	795
7	750	h	165	270	369	493	491	697
		$h + h_0$	315	420	519	643	641	847
8	770	h	176	288	421	527	524	745
		$h + h_0$	326	438	571	677	674	895
9	775	h	187	306	474	554	556	790
		$h + h_0$	337	456	624	704	706	940

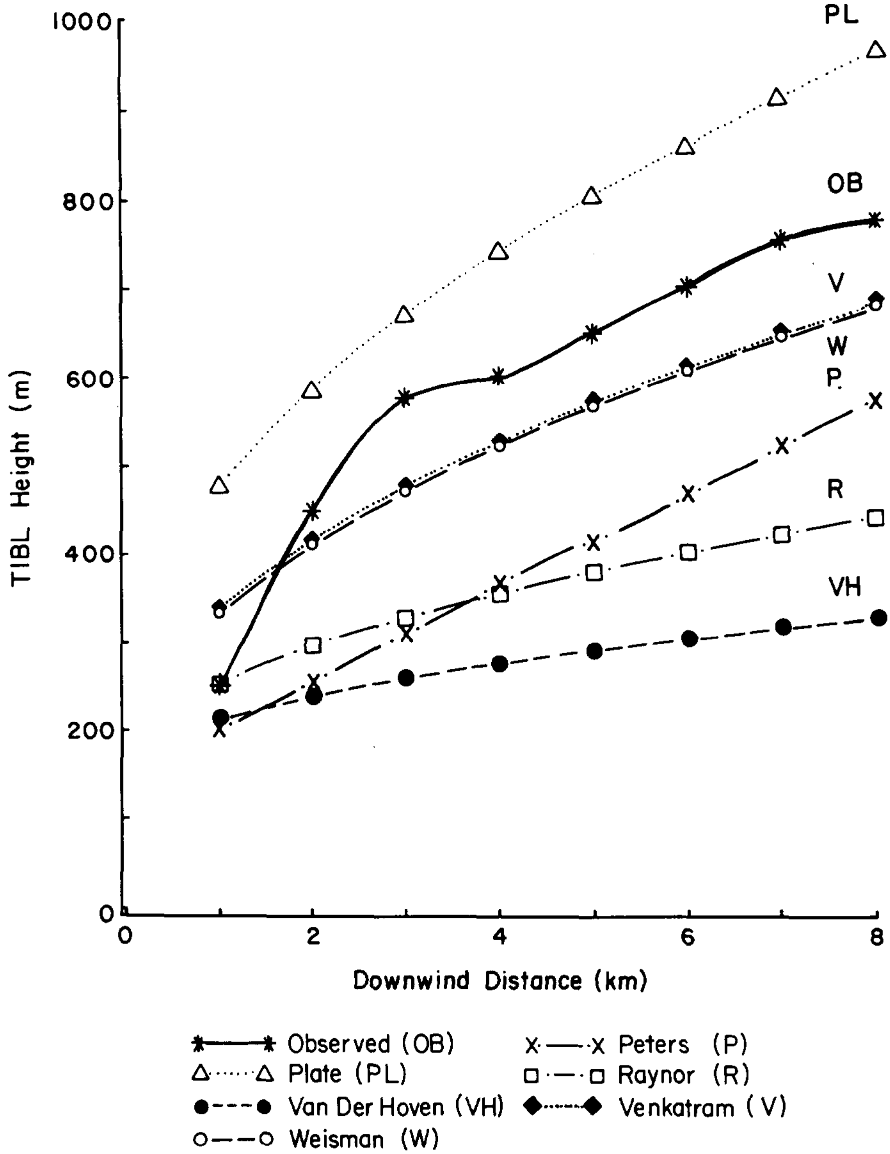

Fig. 8. Predicted and observed TIBL values for the onshore neutral BNL BL#6 case.

temperature profile. Table VI gives an interesting comparison of the predicted values of the TIBL with and without h_0. The TIBL prediction equations without h_0 greatly underpredict the TIBL.

The TIBL grew very rapidly for this case after 2 km because of the development of intense overland convection. Figure 8 shows the TIBL height with downwind distance X. Weisman's formulation (Equation (17)) with the h_0 modification predicts the best, together with Venkatram's formulation (Equation (7)). It is possible that Venkatram's formulation predicts better values than the previous case because of the relatively uniform winds in the TIBL. The average h difference between the Weisman formulation and the Venkatram formulation was about 10 m which is within the observational error.

Two typical cases of different upwind stabilities have indicated mixed results of the predictive capabilities of various equations. Statistical evaluation of these equations with the two data bases will be the subject of the succeeding sections.

6.2. Statistical Evaluation of TIBL Models

A number of studies have presented various criteria for evaluation of the performance of air quality models (EPA, 1981, Fox, 1981). These studies recommend various protocols or procedures for model comparison. The core of a model evaluation protocol is the presentation of various statistical methods which are used to judge model performance.

We have modified the recent air quality model statistical comparison scheme presented by Hanna (1983) to evaluate the various TIBL equations in this paper. The method involves assignment of points based on the results of three statistical tests. The model with the highest total points is considered to be the best TIBL predictor.

Statistical methods used in this scheme are the t and the F tests and the correlation coefficient. The scheme is based on the relationship between bias, variance and correlation. A predicted value equals an observed value if (1) the bias is zero (2) the variance of predicted minus observed values is equal to zero and (3) the predicted vs observed correlation coefficient is one.

The first statistical method (t method) examines the departure of a mean value from some test mean value (see for example, Neville and Kennedy, 1969; Panofsky and Brier, 1968):

$$t = \left(\frac{\overline{\chi} - \mu}{S}\right)\sqrt{n - 1} \tag{23}$$

where

$\overline{\chi}$ = Sample mean.

μ = Hypothetical mean.

n = Sample size.

S = Variance.

The t method can be directly applied to the TIBL evaluation by replacing Equation (23) by:

$$t = \frac{(\overline{O} - \overline{P})}{\sqrt{S_0^2 + S_P^2}}\sqrt{n - 1} \tag{24}$$

where

$\overline{O}$ = Mean of observed TIBL values.

$\overline{P}$ = Mean of the predicted TIBL values for a given equation.

S_0^2 = Variance of observed TIBL values.

S_P^2 = Variance of predicted TIBL values for a given equation.

The $(\overline{O} - \overline{P})$ term itself is called the bias or residual of the model and is quite useful in determining directional model variation from observed values (Fox, 1981).

Equation (24) represents the ratio of the residuals to the variances. The t value therefore shows how the bias is related to the scatter. Ideally if $\overline{O}$ is equal to $\overline{P}$, t will equal 0.

The scoring system for Equation (24) (Hanna, 1983) is based on the actual numerical t value as opposed to the significance level of t. The point assignment was selected to be:

$$\text{Points} = 1 \text{ if } |t| \leqslant 1$$
$$\text{Points} = t \text{ if } |t| > 1.$$

Although this scheme is rather subjective, it is uniformly applied to all the cases.

The second statistical method (F method) examines the ratio of the observed to predicted variance. Ideally, this ratio should be equal to one which means that there is no variability between the observed variances and the predicted variances.

Typically the F method is given as the ratio of the variances:

$$F = \frac{S_x^2}{S_y^2}. \tag{25}$$

The F method can be directly applied to the TIBL evaluation by changing Equation (25) to:

$$F = \max\left(\frac{S_0^2}{S_p^2}, \frac{S_p^2}{S_0^2}\right). \tag{26}$$

The scoring system for Equation (26) based on the actual F value (Hanna, 1983) is:

$$\text{Points} = F^{-1}.$$

The third statistical method (correlation) used a Pearson product moment correlation equation:

$$r = \sum_{i=1}^{n} \frac{(P - \overline{P})(O - \overline{O})}{nS_pS_0} \tag{27}$$

where r = correlation coefficient. The correlation value is then transformed into a normal value (Snedecor and Cochran, 1971) using the relation:

$$z(r) = 0.5 \ln \frac{(1 + r)}{(1 - r)}. \tag{28}$$

The standard deviation of z can be written as:

$$\sigma_z = \frac{1}{\sqrt{n - 3}}. \tag{29}$$

Assuming a significance level of 0.05 (which corresponds to a normal z value of 0.96), the relationship,

$$1.96 = \frac{z(r)}{\sigma_z} \tag{30}$$

can be used to obtain z. The z value can then be used to determine r (from Equation (28)).

An R value is then defined to be (Hanna, 1983):

$$R = z(r)\sqrt{n-3}. \tag{31}$$

Individual R values are then calculated based on the specific correlation values (r). The scoring system for Equation (31) is based on the critical R value, $R_c = 4$. The point assignment is:

$$\begin{array}{lll} \text{Points} = R/4 & \text{if} & R \leqslant R_c \\ \text{Points} = 1 & \text{if} & R > R_c \\ \text{Points} = 0 & \text{if} & r \leqslant 0. \end{array}$$

Notice that the most points are assigned to models which have an r significantly greater than 0.

Since the t method is a ratio between bias and scatter, the possibility exists that an equation or model with low mean bias (small numerator term) and high scatter (large denominator term) may receive more points than an equation with less scatter. The F method, however, would account for the differences in scatter. In our evaluation, we have weighted different statistical methods as follows: t method 1.0; F method 0.5; R method 0.5.

The most significant statistical method in comparing model differences is the t method since it directly uses the $(\overline{O} - \overline{P})$ term. This method was therefore given two times as much weight as the other two methods. Observed minus predicted TIBL values and appropriate mean values were generated for each observation. Various statistical parameters (i.e., S_0^2, S_p^2 and r) were determined from basic statistical equations.

The maximum score a model could receive is 2 (one point for the t method and 0.5 points each for the F and R methods). The $(\overline{O} - \overline{P})$ values themselves were also examined independently as a secondary method. As discussed before, the data were classified according to various meteorological parameters to examine the meteorological condition best suited for different models. The non-categorized cases are presented in the next section with the data categorized by wind speed and stability presented in succeeding sections.

6.3. Non-categorized Data Analysis

An analysis of both data bases was undertaken to determine the best predictive equation. The mean $(\overline{O} - \overline{P})$ values and their rankings appear in Table VII. The points and subsequent rankings based on the method outlined above also appear in Table VII.

The $(\overline{O} - \overline{P})$ values themselves indicate that the Weisman equation has the least deviation from the observed value while the Venkatram formulation shows the most deviation from the observed value. Table VII also shows that all equations except Van der Hoven overpredict. The point rankings are consistent with the initial $(\overline{O} - \overline{P})$ values except for those of Raynor *et al.* and Peters (rank of 3 and 5 reversed). The lesser rank of Raynor *et al.*'s equation for the point scheme is probably because of the inclusion of a scatter measure (Raynor *et al.*'s equation has wide scatter for near-neutral cases). It appears that the equations without a $T_L - T_W$ term (Weisman, Van der Hoven, and Plate) on the whole outperformed the equations with a $T_L - T_W$ term.

TABLE VII

Non-Categorized Data

	$(\overline{O}-\overline{P})$	Rank
(a) $(\overline{O}-\overline{P})$ Values		
Weisman (1976)	−29	1
Van der Hoven (1967)	133	2
Raynor *et al.* (1975)	−189	3
Plate (1971)	−190	4
Peters (1975)	−247	5
Venkatram (1977)	−633	6

	$(\overline{O}-\overline{P})$	Rank
(b) Point Scheme Values		
Weisman (1976)	1.61	1
Van der Hoven (1967)	0.886	2
Peters (1975)	0.858	3
Plate (1971)	0.772	4
Raynor *et al.* (1975)	0.769	5
Venkatram (1977)	0.627	6

The Van der Hoven (1967) formulation seems to do surprisingly well. The equation contains $\Delta\theta$ in the denominator. This term may account for much of the success of the equation. The term does not depend directly on Δz over the water. By not being a function of Δz, the term is usually greater than 0.5 K. This somewhat mitigates the problem of having $d\theta/dz \rightarrow 0$ for near-neutral cases. The equation generally underpredicts TIBL height. Peters' formulation (Equation (10)) was ranked 3th in the points method and 5th in the $(\overline{O} - \overline{P})$ method. This lower ranking is probably caused by the linear relationship. Also, the equation predicting linear growth of TIBL height with distance cannot be used at large downwind distances (Peters, 1975).

The Raynor *et al.* (Equation (2)), Plate (Equation (16)) and Venkatram (Equation VII) formulations received lesser rankings. Apparently, the Raynor *et al.* and Plate formulations are directly affected by large predicted departures from the observed values because of the influence of the unstable and isothermal cases.

The Venkatram equation performs the worst since it relies on a fixed entrainment factor (F) and mixed-layer wind u_m.

6.4. Analysis of Combined Data Bases – by Wind Category

The combined data base was divided into two wind categories ($U1$ and $U2$) so that we could examine any significant changes between the non-categorized and the categorized method. Classification by wind speed gives us some linkage to the different mesoscale and synoptic scale conditions present (for example, higher winds under sea breeze conditions) in the study areas.

TABLE VIII

Wind Categorized Data

	$(\bar{O}-\bar{P})$	Rank		$(\bar{O}-\bar{P})$	Rank
		Category $U1$ ($U \leqslant 4$ m s^{-1})			
(a) $(\bar{O}-\bar{P})$ Values			(b) Point Scheme Values		
Van der Hoven (1967)	117	1	Weisman (1976)	0.970	1
Weisman (1976)	−139	2	Van der Hoven (1967)	0.907	2
Raynor *et al.* (1975)	−237	3	Raynor *et al.* (1975)	0.761	3
Plate (1971)	361	4	Peters (1975)	0.748	4
Peters (1975)	−520	5	Plate (1971)	0.743	5
Venkatram (1977)	−819	6	Venkatram (1977)	0.651	6
		Category $U2$ ($U \leqslant 4$ m s^{-1})			
(c) $(\bar{O}-\bar{P})$ Values			(d) Point Scheme Values		
Plate (1971)	−21	1	Raynor *et al.* (1975)	1.285	1
Peters (1975)	23	2	Plate (1971)	1.235	2
Weisman (1976)	79	3	Weisman (1976)	1.053	3
Raynor *et al.* (1975)	−142	4	Peters (1975)	0.855	4
Van der Hoven (1967)	149	5	Van der Hoven (1967)	0.811	5
Venkatram (1977)	−510	6	Venkatram (1977)	0.552	6

Category $U1$ contained 101 observations and included wind speeds of 4.0 m sec^{-1} or less. Category $U2$ contained 102 observations and included wind speeds greater than 4.0 m sec^{-1}. Lower wind speeds would generally tend to near-free convection and higher TIBL heights as shown by Raynor *et al.* (1979).

Table VIII (a), (b) shows the $U1$ $(\bar{O} - \bar{P})$ values, their rankings and the point values along with their rankings. It appears that the formulation by Weisman performs best under low wind conditions. It is interesting to note that the top three rankings are fairly consistent with the non-categorized analysis. Venkatram's formulation does very poorly, overpredicting on the average by 819 m. The formulation is also ranked last in the point scheme. This may be because mixed-layer mean wind U_m is used in his equation. As discussed in a previous section, conditions within the TIBL appear to be far from well-mixed for stable upwind conditions.

Table VIII(c), (d) shows the $(\bar{O} - \bar{P})$ values, their rankings and the point values with their rankings for category $U2$. The Van der Hoven formulation is consistently underpredicting the TIBL height for both the wind speed categories. The formulations of Peters and Weisman now underpredict the TIBL height.

It appears that the Raynor *et al.* equation has the best formulation in higher wind speeds based on the point scheme. However, the Plate equation has the closest to zero $(\bar{O} - \bar{P})$ value. As mentioned previously, this discrepancy is accounted for because the scatter and correlation are not included in the $(\bar{O} - \bar{P})$ method. Once again, Venkatram's formulation has lowest ranking.

The improvement in Peters' equation is surprising since there is an inverse relationship between wind speed and TIBL height (higher wind speeds result in lower TIBL heights). The low $(\bar{O} - \bar{P})$ difference, however, is mitigated by the scatter and correlation determinations in the point scheme.

TABLE IX

Stability Categorized Data

Stability S1 (Unstable) $N = 9$	$(\overline{O} - \overline{P})$	Rank
(a) $(\overline{O} - \overline{P})$ Values		
Weisman (1976)	64	1
Venkatram (1977)	66	2
Plate (1971)	164	3
Peters (1975)	199	4
Raynor *et al.* (1979)	244	5
Van der Hoven (1967)	330	6
(b) Point Scheme Values		
Weisman (1976)	1.762	1
Venkatram (1977)	1.759	2
Plate (1971)	1.511	3
Peters (1975)	1.247	4
Raynor *et al.* (1979)	0.847	5
Van der Hoven (1967)	0.720	6

Stability S2 (near-neutral) $N = 51$	$(\overline{O} - \overline{P})$	Rank
(b) $(\overline{O} - \overline{P})$ Values		
Raynor *et al.* (1974)	2	1
Van der Hoven (1967)	106	2
Venkatram (1977)	−237	3
Weisman (1976)	−388	4
Plate (1971)	−712	5
Peters (1975)	−1109	6
(d) Point Scheme Values		
Van der Hoven (1967)	1.243	1
Raynor *et al.* (1979)	1.213	2
Peters (1975)	0.762	3
Weisman (1976)	0.730	4
Plate (1971)	0.674	5
Venkatram (1977)	0.488	6

Stability S3 (isothermal) $N = 72$	$(\overline{O} - \overline{P})$	Rank
(e) $(\overline{O} - \overline{P})$ Values		
Plate (1971)	−53	1
Weisman (1976)	72	2
Peters (1975)	75	3
Van der Hoven (1967)	139	4
Raynor *et al.* (1974)	−547	5
Venkatram (1977)	1442	6
(f) Point Scheme Values		
Plate (1971)	1.562	1
Weisman (1976)	1.497	2
Van der Hoven (1967)	1.025	3
Peters (1975)	0.998	4
Raynor *et al.* (1979)	0.631	5
Venkatram (1977)	0.626	6

Stability S4 (inversion) $N = 71$	$(\overline{O} - \overline{P})$	Rank
(g) Point Scheme Values		
Raynor *et al.* (1974)	−19	1
Peters (1975)	−30	2
Plate (1971)	42	3
Weisman (1976)	114	4
Van der Hoven (1967)	121	5
Venkatram (1977)	274	6
(h) Point Scheme Values		
Raynor *et al.* (1979)	1.972	1
Peters (1975)	1.351	2
Plate (1971)	1.347	3
Weisman (1976)	0.834	4
Venkatram (1977)	0.789	5
Van der Hoven (1967)	0.729	6

6.5. Analysis of Combined Data Bases – by Stability Category

The combined data base was divided into four stability categories based on over-water stability labelled S1, S2, S3, and S4. The division of each stability category is as follows:

$$\text{S1:}\ \frac{dT}{dz} \leqslant -0.012\ \text{K m}^{-1}\ \text{(fairly unstable)}$$

$$\text{S2:}\ -0.012 < \frac{dT}{dz} \leqslant -0.005\ \text{K m}^{-1}\ \text{(near neutral)}$$

$$\text{S3:}\quad -0.005 < \frac{\mathrm{d}T}{\mathrm{d}z} \leqslant -0.005\ \mathrm{K\ m^{-1}}\ \text{(isothermal)}$$

$$\text{S4:}\quad \frac{\mathrm{d}T}{\mathrm{d}z} > +0.005\ \mathrm{K\ m^{-1}}\ \text{(stable).}$$

It is important to note that category S1 contained only nine observations. Conclusions based on this category should therefore be used with some caution. Category S3 was observed only in the BNL data base. Table IX gives the number of observations (N), the $(\bar{O} - \bar{P})$ values, the point values and the rankings for all four stability classifications.

Weisman's (1976) formulation is shown to be the best for the limited S1 category. The Venkatram equation also performs well based on both the point scheme and averaged $(\bar{O} - \bar{P})$ values for the unstable S1 case. The reason for the second best ranking may be associated with the mixed-layer assumption that Venkatram makes under unstable conditions. The Van der Hoven equation appears to be the least desirable formula for the unstable S1 case.

For the neutral case, the Raynor *et al.* formulation has an averaged $(\bar{O} - \bar{P})$ value close to zero; however, the correlation and scatter of the values are large enough so that the point scheme reflects a rank of two. Venkatram's formula is ranked last in the S2 case point scheme values (Table IXd) which is inconsistent with this high ranking under condition S1, given the well-mixed assumption. The linear equation of Peters does poorly (3rd ranking in the points scheme) in this case.

Plate's formulation together with Weisman's formulation predict the best for the isothermal case. Raynor *et al.*'s formulation is ranked 5th for the S3 case since $\mathrm{d}T/\mathrm{d}z \to 0$ in the denominator. The equation overpredicts for this category.

Finally, for the S4 inversion case, Raynor's formula appears to be the best with very low $(\bar{O} - \bar{P})$ values (− 19) and high point scheme rankings (1st). Under S4 conditions, the contributing terms in the Raynor *et al.* equation is probably the $T_L - T_W$ term which would be a large number. We could not account for the high ranking of the Peters equation.

7. Conclusions

The ability to predict the TIBL height based on either direct or indirect meteorological measurements is clearly a necessary prerequisite to successful dispersion modeling in coastal areas. A difference of 120 m between two TIBL heights could mean a difference of 7 km in the location of the fumigation zone. This would have a significant impact on ground-level concentration distributions.

Six different TIBL formulations were identified in the literature. They were compared and statistically evaluated using two data bases. One was from eastern Long Island and the other from Kashimaura, Japan. Five other data sets were identified from the literature but lacked important information such as land and water temperatures and overwater thermal stabilities.

The models were evaluated with the entire data set and also according to wind speed and overwater thermal stability. The statistical methods consisted of performing t, F, and R tests on predicted values using the observations of TIBL height. A point scheme similar to Hanna (1983) was used for the quantitative evaluation purposes. A total of 29 individual experiments and 203 TIBL values were used for the statistical comparison.

The formulation of Weisman (1976) appears overall to predict the TIBL the best. Categorization by stability also indicated that Weisman's equation performs best under unstable and isothermal conditions. The equations were also independently evaluated using a statistical ranking scheme suggested by Willmott (1982, 1984). The rankings were essentially the same.

These results are based on limited data sets. There is a clear need for further comprehensive measurements of important meteorological parameters identified in this paper to understand better the formation of the TIBL and the accompanying fumigation processes in a coastal region.

Acknowledgements

We thank Gil Raynor (Brookhaven National Laboratory) and Minoru Gamo (National Research Institute for Pollution and Resources, Japan) for providing the TIBL data. We also thank Bob Paine (Environmental Research and Technology, Inc.) for several helpful discussions. This work was supported by the Source Receptor Analysis Branch, Office of Air Quality Planning and Standards, Environmental Protection Agency, Durham, North Carolina.

References

Anthes, R. A.: 1978, 'The Height of the PBL and the Production of Circulation in a Sea Breeze Model', *J. Atm. Sci.* **35**, 1231–1239.

Ball, F. K.: 1960, 'Control of Inversion Height by Surface Heating', *Quart. J. Roy. Meteorol. Soc.* **86**, 483–494.

Betts, A. K.: 1973, 'Non Precipitating Cumulus Convection and its Parameterization', *Quart J. Roy. Meteorol. Soc.* **99**, 170–196.

Elliott, W. P.: 1958, 'The Growth of the Atmospheric Internal Boundary Layer', *Trans. Amer. Geophys. Union* **39**, 1048–1067.

Environmental Protection Agency: 1981, *Interim Procedures for Evaluating Air Quality Models*, Office of Air Quality Planning and Standards, Durham, NC.

Fox, D. G.: 1981, 'Judging Air quality Model Performance. A Summary of the AMS Workshop on Dispersion Model Performance', *Bull. Am. Meteorol. Soc.* **62**, 599–609.

Fritts, T. W., Starheim, F. J., and Deihl, B. J.: 1980, *A Formulation for Defining the Development of the TIBL in Sea Breeze Flows*, Preprints: Second Conf. on Coastal Meteorology AMS, Los Angeles, 147–150.

Gamo, M. S.: 1981, *A Study on the Structure of the Free Convective Internal Boundary Layer During the Sea Breeze*. Report of the National Research Institute for Pollution and Resources (Japan) # 19, 89 pp.

Gamo, M., Yamamoto, S., and Yokoyama, O.: 1982, 'Airborne Measurements of the Free Convective Internal Boundary Layer During the Sea Breeze', *J. Meteorol. Soc. Japan* **60**, 1284–1298.

Gamo, M., Yamamoto, S., Yokoyama, O., and Yashikado, H.: 1983, 'Structure of the Free Convective Internal Boundary Layer Above the Coastal Area'. *J. Meteorol. Soc. Japan* **61**, 110–124.

Hanna, S. R.: 1983, *A Simplified Scoring System for Air Quality Models*. Paper 8336.6. Annual Air Pollution Control Assoc. Meeting, Atlanta, GA June.

Kerman, B. R., Mickle, R. E., Portelli, R. V., and Trivett, N. B.: 1982, 'The Nanticoke Shoreline Diffusion Experiment, June 1978-II-Internal Boundary Layer Structure', *Atmos. Env.* **16**, 423–437.

Lui: 1977, *A Literature Review of Boundary Layer Models*, Report #79573K Ontario Hydro Inc. 26 pp.

Lyons, W. A.: 1975, *Turbulent Diffusion and Pollutant Transport in Shoreline Environments*. Lectures on Air Pollution and Environmental Impact Analysis, AMSë Boston 136–208.

Lyons, W. A.: 1977, *Mesoscale Air Pollution Transport in Southeast Wisconsin*, EPA 600/4-77-010. U.S. Environmental Protection Agency.

Lyons, W. A. and Cole, H. S.: 'Fumigation and Plume Trapping on the Shores of Lake Michigan During Stable Onshore Flow', *J. App. Meteorol.* **12**, 494–510.

Lyons, W. A., Keen, C. S., and Schuh, J. A.: 1983, *Modeling Mesoscale Diffusion and Transport Processes for Releases within Coastal Zones during Land/Sea Breezes*. United States Nuclear Regulatory Commission. NUREG/CR3542.

Misra, P. K.: 1980, 'Dispersion From Tall Stacks Into a Shoreline Environment', *Atmos. Env.* **14**, 396–400.

Misra, P. K. and Onlock: 1982, 'Modelling Continuous Fumigation of the Nanticoke Generating Station Plume', *Atmos. Env.* **16**, 479–489.

Neville, A. M. and Kennedy, J. B.: 1964, *Basic Statistical Methods for Engineers and Scientists*, International Company, 325 pp.

Panofsky, H. A. and Brier, G. W.: 1968, *Some Applications of Statistics to Meteorology*, Pennsylvania State University, 224 pp.

Peters, L. K.: 1975, 'On the Criteria for the Occurrence of Fumigation Inland From a Large Lake', *Atmos. Env.* **9**, 809–816.

Plate, E. J.: 1971, *Aerodynamic Characteristics of Atmospheric Boundary Layers*, United State Atomic Energy Commission, 190 pp.

Portelli, R. B.: 1982, 'The Nanticoke Shoreline Diffusion Experiment, June 1978 1, Experimental Design and Program Overview', *Atmos. Env.* **16**, 413–421.

Prophet, D. T.: 1961, 'Survey of the Available Information Pertaining to the Transport and Diffusion of Airborne Material Over Ocean and Shoreline Complexes', *Tech. Rep.* No. **89**, Aerosol Lab, Stanford Univ. CA.

Raynor, G. S., Michael, P., Brown, R. M., and SethuRaman, S.: 1975, Studies of Atmospheric Diffusion From a Nearshore Oceanic Site', *J. App. Meteorol.* **14**, 1080–1094.

Raynor, G. S., SethuRaman, S., and Brown, R. M.: 1979, 'Formation and Characteristics of Coastal Internal Boundary Layers During Onshore Flows', *Boundary Layer Meteorol.* **16**, 487–514.

Schuh, J. A.: 1975, 'A Mesoscale Model of Continuous Shoreline Fumigation and Lid Trapping in a Wisconsin Shoreline Environment', *Rep. No.* 27, Center for Gr. Lakes Studies, Univ. of Wisconsin-Mil.

SethuRaman, S. and Brinkman, D.: 1983, *On the Variation of Turbulence Within the TIBL*, Preprints: Sixth Symposium on Turbulence and Diffusion, AMS, Boston, March, 287–289.

SethuRaman, S.: 1982, *Observations of the Boundary Layer Wind Structure Near the Land-Sea Interface*, Prepints: First International Conference on Meteorology and Air-Sea Interaction of the Coastal Zone, May 10–14, 1982, The Hague, Netherlands.

SethuRaman, S., Raynor, G. S., and Brown, R. M.: 1982, *Variation of Turbulence in a Coastal Thermal Internal Boundary Layer*, Prepints: Third Joint Conference on the Applications of Air Pollution Meteorology, American Meteorological Society, Boston, MA.

Snedecor, G. W. and Cochran, W. G.: 1971, *Statistical Methods*, Sixth Edition. Iowa State Press, 593 pp.

Van der Hoven, I.: 1967, 'Atmospheric Transport and Diffusion at Coastal Sites', *Nuc. Safety* **8**, 490–499.

Van Dop, H., Steenkist, R., and Nieuwstadt, F. T. M.: 1979, 'Revised Estimates for Continuous Shoreline Fumigation', *J. App. Meteorol.* **18**, 133-137.

Venkatram, A.: 1977, 'A Model of Internal Boundary Layer Development', *Boundary-Layer Meteorol.* **11**, 419–437.

Weisman, B.: 1976, 'On the Criteria for the Occurrence of Fumigation Inland From a Large Lake – A Reply', *Atmos. Env.* **12**, 172–173.

Willmott, C.: 1982, 'Some Comments on the Evaluation of Model Performance', *Bull. Amer. Meteorol. Soc.* **63**, 1309–1313.

Willmott, C.: 1984, 'On the Evaluation of Model Performance in Physical Geography in Spatial Statistics and Models', in G. Gaile and C. Willmott (eds.), *Spatial Statistics and Models*, D. Reidel, pp. 443–460.